ACS APPLIED MATERIALS & INTERFACES

Letter

www.acsami.org

Patterning of Magnetic Thin Films and Multilayers Using Nanostructured Tantalum Gettering Templates

Wenlan Qiu,[†] Long Chang,[‡] Dahye Lee,[†] Chamath Dannangoda,[§] Karen Martirosyan,[§] and Dmitri Litvinov*[,†,‡]

[†]Materials Science & Engineering and [‡]Electrical & Computer Engineering, University of Houston, Houston, Texas 77204, United States

[§]Department of Physics & Astronomy, University Texas at Brownsville, Brownsville, Texas 78520, United States

ABSTRACT: This work demonstrates that a nonmagnetic thin film of cobalt oxide (CoO) sandwiched between Ta seed and capping layers can be effectively reduced to a magnetic cobalt thin film by annealing at 200 °C, whereas CoO does not exhibit ferromagnetic properties at room temperature and is stable at up to ~400 °C. The CoO reduction is attributed to the thermodynamically driven gettering of oxygen by tantalum, similar to the exothermic reduction−oxidation reaction observed in thermite systems. Similarly, annealing at 200 °C of a nonmagnetic $[CoO/Pd]_N$ multilayer thin film sandwiched between Ta seed and Ta capping layers results in the conversion into a magnetic $[Co/Pd]_N$ multilayer, a material with perpendicular magnetic anisotropy that is of interest for magnetic data storage applications. A nanopatterning approach is introduced where $[CoO/Pd]_N$ multilayers is locally reduced into $[Co/Pd]_N$ multilayers to achieve perpendicular magnetic anisotropy nanostructured array. This technique can potentially be adapted to nanoscale patterning of other systems for which thermodynamically favorable combination of oxide and gettering layers can be identified.

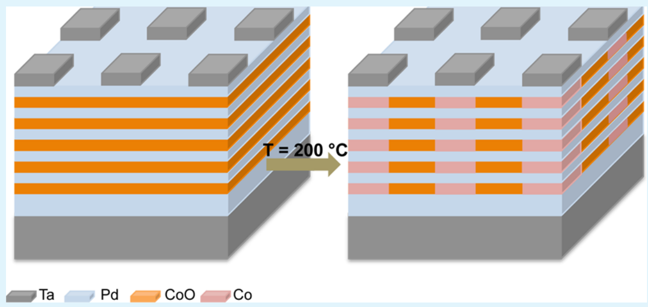

KEYWORDS: *cobalt oxide, Co/Pd multilayer, low temperature annealing, nanoscale patterning, bit-patterned media*

Nanoscale patterning of magnetic metals and their alloys remains a significant challenge because of the lack of reactive-ion etching chemistries producing volatile compounds of magnetic elements.[1,2] Lithography patterning is typically accomplished either via a lift-off process, ion milling, or wet etching, all lacking the needed fidelity to achieve the high resolution and high pattern density because of fabrication issues such as fencing, shadowing, edge damage, and redeposition.[2,3] Alternatively, electrochemical deposition may circumvent these fabrication issues and produce high aspect ratio structures, but it is difficult to make complex multilayers.[3]

This work demonstrates local reduction of nonmagnetic CoO and nonmagnetic $[CoO/Pd]_N$ multilayers, effectively achieving magnetic nanostructures without the physical removal of magnetic materials. The process takes advantage of the exothermic reduction of the thin film CoO layer sandwiched between tantalum layers annealed at 200 °C. For reference, cobalt oxide is stable up to approximately 400 °C.[4] In this energetically favorable reaction, tantalum is oxidized in the process via $5CoO + 2Ta = 5Co + Ta_2O_5$ (−1.15 kJ/g). This exothermic reduction−oxidation reaction is similar to the ones exhibited by thermite nanocomposites.[5]

CoO thin films and $[CoO/Pd]_N$ multilayers are deposited using an AJA ATC 2200 ultrahigh vacuum DC magnetron sputtering system with a base pressure of 5×10^{-8} Torr. The process pressure for all films is 5×10^{-3} Torr. CoO films are deposited by reactive magnetron sputtering with argon (35 sccm) and oxygen (5 sccm); all other materials (Co, Pd, Ta) are deposited by sputtering with argon (35 sccm). Patterns are produced on the films by exposing HSQ resist using a JEOL JBX 5500FS eBeam Writer. The resist pattern is transferred into the film via argon ion milling and examined by FEI XL-30FEG scanning electron microscope (SEM). A MicroMag alternating gradient magnetometer (AGM) and a polar magneto-optical Kerr effect (PMOKE) magnetometer are used to measure the saturation magnetization (M_s) and switching properties, respectively. X-ray photoelectron spectroscopy (XPS) data were collected using a Physical Electronics model 5700 XPS instrument at a residual pressure of 5×10^{-9} Torr or better. A monochromatic Al-kα X-ray (1486.6 eV) at 350 W were used as a source of photoelectrons. The photoelectrons were collected at a 45° take off angle with respect to the 0.8 mm analyzed area of sample and the collection solid cone was 5°. All spectra were recorded with applying a pass energy of 11.75 eV that causes an energy resolution of better than 0.51 eV.

To study the role of Ta in this process, a 10 nm CoO thin film is sandwiched between a 15 nm Ta seed layer and a 2.5 nm

Received: December 22, 2014
Accepted: March 11, 2015
Published: March 11, 2015

DOI: 10.1021/am5090463
ACS Appl. Mater. Interfaces 2015, 7, 6014−6018

capping layer. The saturation magnetization of the 10 nm CoO thin film annealed at different temperatures for 5 min is shown in Figure 1a. It is observed that the M_s of CoO is approximately 0 emu/cc and increases to approximately 1300 emu/cc at a temperature as low as 200 °C. The M_s of annealed CoO approaches the M_s of sputtered Co thin film as the temperature approaches 200 °C; no changes were observed at annealing temperatures beyond 200 °C. The hysteresis loop of CoO thin film annealed at 200 °C for 5 min is shown in Figure1b.

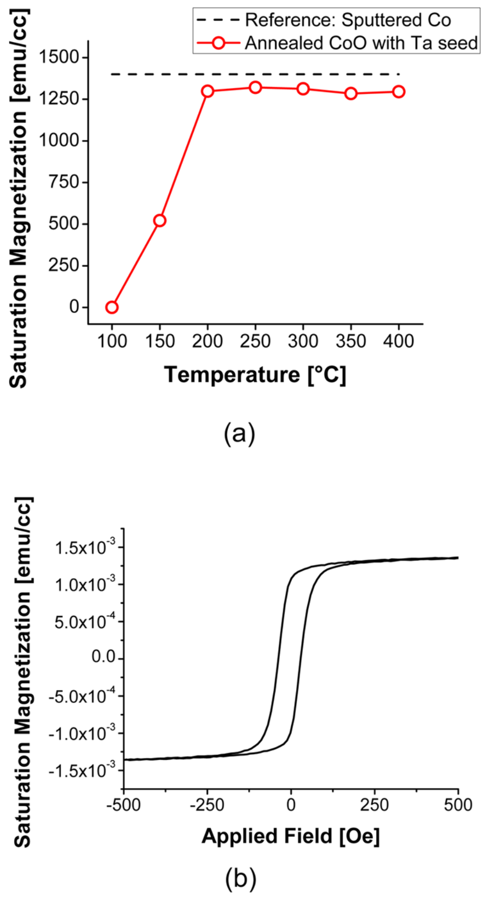

Figure 1. (a) Saturation magnetization of annealed CoO thin film sandwiched between Ta seed and capping layers depending on annealing temperature in air. An emergence of magnetization is observed for annealing at 150 °C and a full conversion is achieved for temperatures above 200 °C. The saturation magnetization of the annealed CoO is comparable to the sputtered Co. (b) Hysteresis loop of annealed CoO thin film.

Driven by the above observation, CoO have been introduced into the Co/Pd multilayer system to further study the fidelity of this low temperature annealing process because individual layer quality and interface environment sensitively determine the perpendicular magnetic anisotropy of Co/Pd multilayer. $[Co/Pd]_N$ multilayers have been studied extensively as a candidate material for high-density magnetic recording, promising areal densities beyond 1 TB/in^2.[6−9] $[Co/Pd]_N$ multilayers exhibit strong perpendicular magnetic anisotropy and high saturation magnetization, tunable through manipulating the seed layer, individual Co and Pd layer thickness, number of layers, and deposition conditions.[8−11]

The deposition parameters for an optimized high magnetic anisotropy $[Co/Pd]_{10}$ multilayer with the following composition Ta(15 nm)/Pd(0.7 nm)/$[Co(0.3\ nm)/Pd(0.7\ nm)]_{10}$/Ta(2.5 nm)[12] were used to deposit Ta/$[CoO/Pd]_{10}$/Ta thin film where oxygen was introduced during Co layers deposition step. As deposited, $[CoO/Pd]_{10}$ multilayers did not exhibit ferromagnetic properties. However, a strong onset of ferromagnetic properties was observed upon annealing the $[CoO/Pd]_{10}$ multilayers in air at ∼200 °C for 5 min, and the hysteresis loop is shown in Figure 2a.

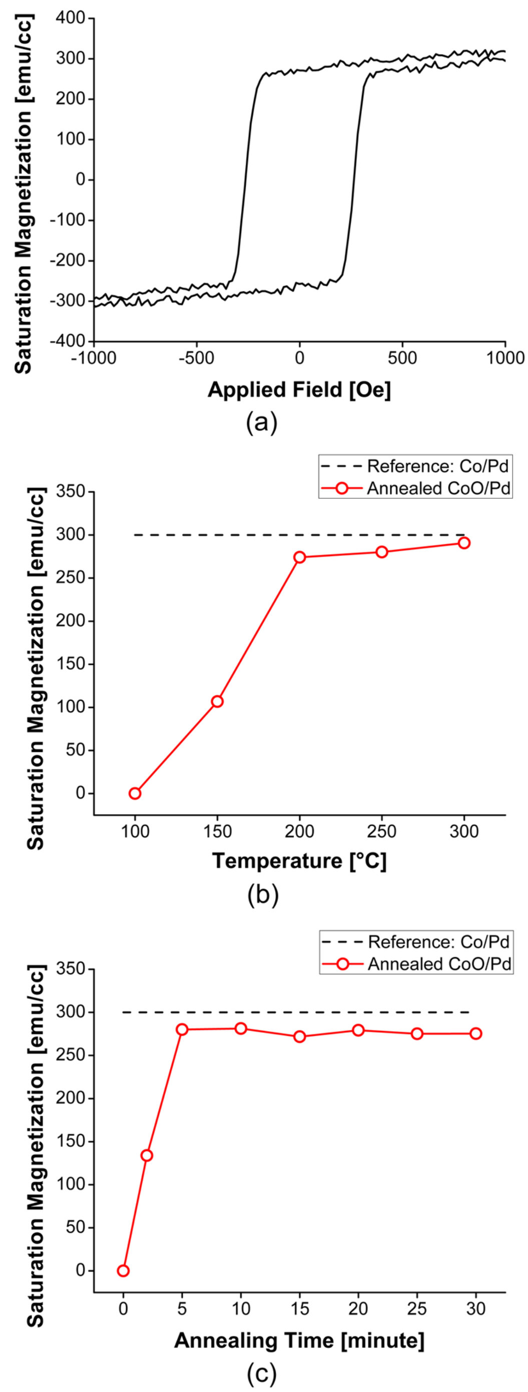

Figure 2. (a) Hysteresis loop of $[CoO/Pd]_{10}$ multilayers annealed at 200 °C for 5 min. The saturation magnetization of annealed $[CoO/Pd]_{10}$ multilayers varies as a function of (b) annealing temperature and (c) annealing time. Nonmagnetic $[CoO/Pd]_{10}$ is completely converted to magnetic $[Co/Pd]_{10}$ by annealing at 200 °C for 5 min or longer.

DOI: 10.1021/am5090463
ACS Appl. Mater. Interfaces 2015, 7, 6014−6018

The M_s of $[CoO/Pd]_{10}$ annealed at 200 °C approached the M_s as that of sputtered $[Co/Pd]_{10}$ as shown in Figure 2b. Because the magnetic properties of Co/Pd multilayer films are controlled by the interfacial effects between Co and Pd layers,[13,14] it is evident that $[CoO/Pd]_{10}$ transforms into to $[Co/Pd]_{10}$. Judging from the M_s of annealed $[CoO/Pd]_{10}$, annealing at temperatures below 200 °C shows a partial conversion of CoO to Co, while annealing at temperatures above 200 °C resulted in a complete conversion, as shown in Figure 2b. Annealing the CoO/Pd film for longer than 5 min at a temperature of 200 °C does not increase the saturation magnetization, as shown in Figure 2c. The significant reduction in annealing temperature from 400 to 200 °C for the conversion of CoO to Co may be attributed to the presence of Ta in the film stack via its gettering property.

To investigate the influence of a Ta layer on this low temperature annealing process in multilayer structure, we replaced the Ta seed layer and capping layer with Pd of the same thickness and performed the same annealing experiments. However, the modified $[CoO/Pd]_{10}$ multilayers did not exhibit ferromagnetic properties at annealing temperatures of up to 400 °C, demonstrating that Ta is responsible for the significantly improved conversion process. We have also determined experimentally that as little as a 4 nm layer of Pd inserted between CoO and Ta serves as an effective barrier against the conversion process.

Further study of Tantalum's role in the conversion process is shown through thermodynamic calculations using the thermochemical computer code HSC Chemistry-7, which includes minimization of the Gibbs free energy subject to mass and energy balances.[15] The software simulates chemical reactions and processes on a thermochemical basis and does not take into account the rates of reactions, heat and mass transfer issues. Nonetheless, HSC code offers powerful calculation methods for studying the effects of different variables on the chemical system at equilibrium and observing the effects on product composition of process variables such as temperature and quantity of raw materials. The dependence of the adiabatic temperature and the equilibrium concentration of solid and liquid phases on the cobalt oxide concentration for the CoO-Ta system is shown in Figure 3. The amount of Ta(S) decreases as

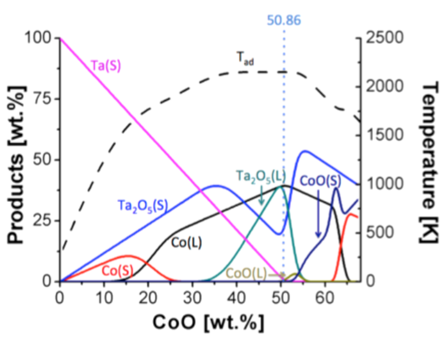

Figure 3. Dependence of the maximum adiabatic temperature and equilibrium concentration of condensed phases on cobalt oxide concentration; (S) and (L) denote solid and liquid states, correspondingly.

CoO increases, until Ta(S) reaches the stoichiometry point where it is being completely consumed as it reacts with CoO. Stoichiometry is reached in the system at 50.86 wt % CoO. The adiabatic temperature rises up to 2150 K with increasing CoO and reaches a plateau between 36–54 wt % CoO. As the adiabatic temperature increases above 1863K, some parts of solid cobalt Co(S) melt to liquid Co(L) as shown in the figure. When the temperature reaches 2150 K, Ta_2O_5 starts to melt. This process continues until CoO reaches the stoichiometry point. When the CoO wt % exceeds the stoichiometry point, excess amounts of CoO can be seen and the adiabatic temperature begins to decrease in the system. The reduced temperature converts liquid Ta_2O_5 to its solid state. Significantly, the thermodynamic calculations confirm the possibility of an exothermic interaction between CoO and Ta without generating any gaseous phases.

XPS analysis was used to further support Ta oxygen gettering from $[CoO/Pd]_5$ multilayers and the conversion of Ta into Ta_2O_5 in the process. $[CoO/Pd]_5$ multilayer and $[Co/Pd]_5$ reference multilayer were grown on Ta(15 nm)/Pd(6 nm) seeds and capped with 2.5 nm Ta films. The multilayers were postdeposition annealed at 200 °C in nitrogen. The corresponding XPS spectra are shown in Figure 4. The larger

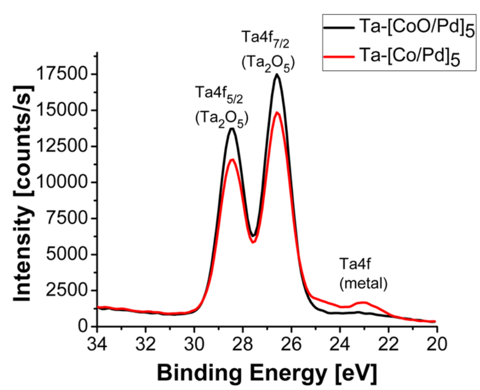

Figure 4. XPS spectra of annealed $[CoO/Pd]_5$ reveals vanishing Ta metal peaks compared to $[Co/Pd]_5$.

amplitude of Ta_2O_5 peaks (Ta $4f_{7/2}$ at 26.7 eV and Ta $4f_{5/2}$ at 28.6 eV) for Ta/Pd/$[CoO/Pd]_5$/Ta film as compared to the Ta/Pd/$[Co/Pd]_5$/Ta reference clearly shows that Ta getters oxygen from the underlying $[CoO/Pd]_5$ multilayer.[16−19] Furthermore, a Ta 4f peak at 23 eV associated with metallic Ta observed in the $[Co/Pd]_5$ reference multilayer is suppressed in the $[CoO/Pd]_5$ film, which is attributed to Ta oxidation.

To further study the magnetic property of annealed $[CoO/Pd]_N$ multilayers, we prepared a set of films consisting of Ta(15 nm)/Pd(0.7 nm)/$[CoO/Pd(0.7\ nm)]_{10}$/Ta(2.5 nm), where the CoO layer thickness was varied from 0.3 to 0.9 nm, whereas the Pd layer thickness was kept constant at 0.7 nm. Electron beam lithography was used to pattern an array of 200 nm square pillars spaced 400 nm apart in HSQ resist. Approximately 200 μm to the side of this array pattern is a large solid square pattern, 500 μm × 500 μm, that serves as a control. The resist pattern was transferred into the entire film stack via argon ion milling. After annealing at 200 °C for 5 min, the switching properties of patterned films were measured using the PMOKE system. It was reported that grains with defects or certain microstructures, called easy switchers, trigger the domain wall motion and are responsible for the low coercivity in Co/Pd thin films.[20] Patterning stops magnetization reversal triggered by domain wall motion, enabling the comparison (even though qualitatively) of the true magnetic anisotropies in the annealed films.

DOI: 10.1021/am5090463
ACS Appl. Mater. Interfaces 2015, 7, 6014−6018

A series of hysteresis loops comparing the switching properties of $[Co/Pd]_{10}$ multilayers, annealed $[CoO/Pd]_{10}$ multilayers and a series of patterned and then annealed $[CoO/Pd]_{10}$ multilayers is shown in Figure 5. A 40° tilted SEM image of the patterned square array is shown in Figure 5 inset. The control pattern does not have a hysteresis loop after patterning, confirming that heat generated from the patterning and milling process is not sufficient to convert the film. After annealing, the control pattern becomes ferromagnetic with a coercivity of approximately 500 Oe. The hysteresis loops of the annealed patterned films have coercivities ranging from 1 to 2.5 kOe. The change in the switching properties of the converted continuous and patterned $[CoO/Pd]_{10}$ multilayers is significant and resembles typical Co/Pd multilayers. The switching performance of the converted CoO/Pd film will likely improve upon further optimization.

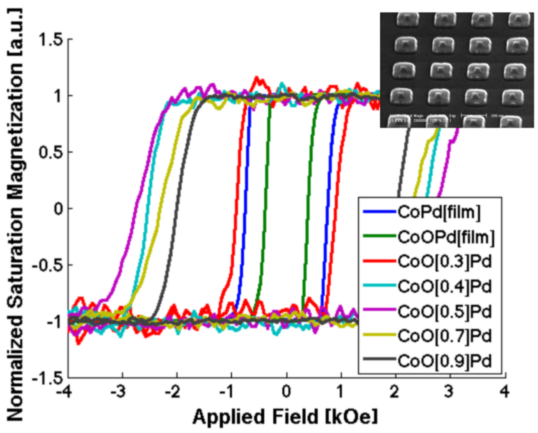

Figure 5. Comparison of the hysteresis loops of $[Co/Pd]_{10}$ film, annealed $[CoO/Pd]_{10}$ film, and annealed $[CoO/Pd]_{10}$ patterned films with different Co layer thickness. A maximum coercivity of approximately 3 kOe was achieved for the patterned film. The inset shows a projected view of the patterned film.

Because Ta is essential for this conversion process, patterning only the Ta capping layer can produce magnetic arrays. A diagram of $[CoO/Pd]_N$ multilayer with patterned square-shaped Ta cap layer is shown in Figure 6. Upon annealing, the Ta islands serve as catalysts for the conversion process, enabling only the CoO in the vicinity to reduce to Co. This process creates ferromagnetic $[Co/Pd]_N$ islands in a matrix of nonmagnetic $[CoO/Pd]_{10}$. For this patterning scheme to work, a 6 nm Pd seed layer is inserted between the Ta seed layer and the $[CoO/Pd]_N$ multilayers to block the reduction of CoO by the Ta seed layer. The absence of Ta directly underneath the $[CoO/Pd]_N$ multilayers resulted in a significant reduction in the magnetization after annealing.

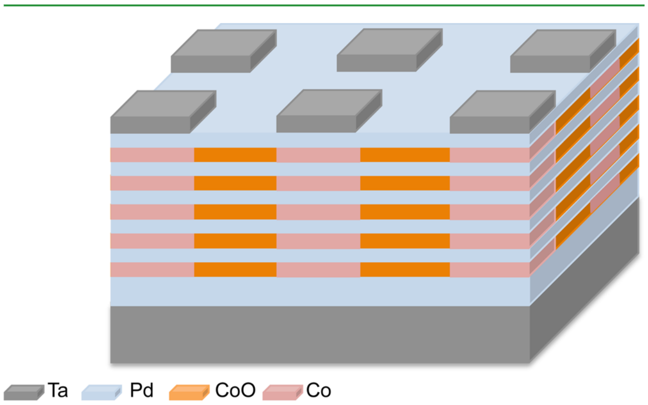

Figure 6. Diagram portrays the BPM fabrication strategy using a patterned Ta capping layer as a catalyst to locally convert CoO/Pd to Co/Pd. Upon annealing, the CoO layers beneath the Ta islands convert to Co resulting in the ferromagnetic Co/Pd islands surrounded by nonmagnetic CoO/Pd film.

The saturation magnetization of annealed CoO(0.3 nm)/Pd(0.7 nm) multilayers on a Ta(15 nm)/Pd(6 nm) seed layer as a function of CoO/Pd bilayer repeats is shown in Figure 7.

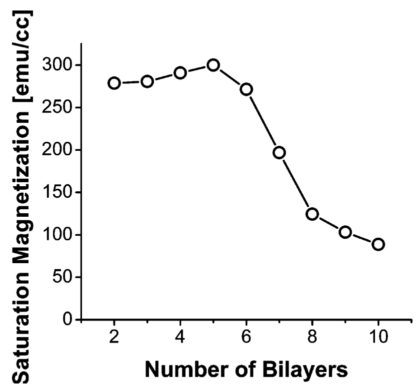

Figure 7. Saturation magnetization of annealed CoO/Pd films varies with the number of bilayer repeats. The magnetization begins to decrease beyond 5 bilayers, implying an incomplete conversion of CoO that is too far from Ta capping layer.

The trend shows that the 2.5 nm of Ta capping layer does not completely convert 10 bilayers of CoO/Pd. At 5 bilayers and below, the saturation magnetization approaches 300 emu/cc, which is equivalent to Co/Pd films. This implies that the effective range for complete conversion of CoO/Pd using Ta is approximately 5 nm. At distances beyond 5 nm, it is hypothesized that the conversion percentage gradually decreases to zero.

Thus, a film stack of Ta(15 nm)/Pd(6 nm)/$[CoO(0.3\ nm)/Pd(0.7\ nm)]_5$/Ta(2.5 nm) was prepared and the Ta cap layer was patterned into an array of 200 nm squares spaced 400 nm apart by electron beam lithography and argon ion milling. Approximately 200 μm to the side of array pattern is a control pattern, 500 μm × 500 μm. After annealing at 250 °C for 5 min, the structure of ferromagnetic $[Co/Pd]_5$ islands in a matrix of nonmagnetic $[CoO/Pd]_5$ film was achieved. A 50 °C higher temperature was necessary to complete the conversion. The $M-H$ loops for these $[Co/Pd]_5$ samples and the control pattern are compared in Figure 8. A larger coercivity in the patterned area (~1150 Oe) than the control pattern (~500 Oe) is observed, confirming that this process can work.

In summary, these results demonstrate that low-temperature annealing can be used to convert nonmagnetic CoO thin films to magnetic Co thin films, and nonmagnetic $[CoO/Pd]_N$ multilayers to ferromagnetic $[Co/Pd]_N$ multilayers, both with optimal saturation magnetization. The annealed $[CoO/Pd]_N$ multilayers have perpendicular magnetic anisotropy and may be a promising candidate for bit-patterned media applications. Significantly, the Ta gettering layer is essential for this conversion process. This new patterning process provides new opportunities for bit-patterned media fabrication and/or other nanoscale patterning of other magnetic systems and

DOI: 10.1021/am5090463
ACS Appl. Mater. Interfaces 2015, 7, 6014−6018

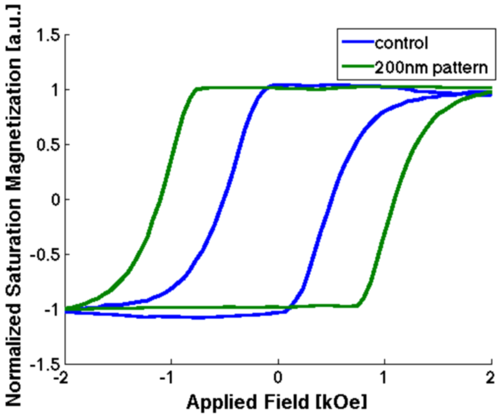

Figure 8. Hysteresis loops comparing the switching property of $[Co/Pd]_5$ multilayers converted from $[CoO/Pd]_5$ multilayers by a 500 μm × 500 μm Ta control pattern and array of 200 nm squares spaced 400 nm apart Ta array pattern. An increased coercivity is observed.

nonmagnetic systems as long as an appropriate exothermic reduction/oxidation reaction can be engineered. Considering our results, it is feasible to fabricate bit-patterned media as suggested in Figure 6. Also, patterning by locally heating can be explored using, for example, heat-assisted magnetic recording (HAMR) head technology to precisely activate the media for recording by creating magnetic islands of Co/Pd.[21−23]

AUTHOR INFORMATION

Corresponding Author

* Dmitri Litvinov, E-mail: Litvinov@uh.edu.

Notes

The authors declare no competing financial interest.

ACKNOWLEDGMENTS

This research is supported in part by NSF Grants CBET-0933140, CMMI-0927786, and ECCS-0926027, and with the resources of the Center for Integrated Bio and Nanosystems. The authors thank Dr. Dieter Weller of Hitachi GST for fruitful discussions.

REFERENCES

(1) Kinoshita, K.; Yamada, K.; Matsutera, H. Reactive Ion Etching of Fe-Si-Al Alloy for Thin Film Head. *IEEE Trans. Magn.* **1991**, *27*, 4888−4890.

(2) Terris, B. D. Fabrication Challenges for Patterned Recording Media. *J. Magn. Magn. Mater.* **2009**, *321*, 512−517.

(3) Lau, J. W.; Shaw, J. M. Magnetic Nanostructures for Advanced Technologies: Fabrication, Metrology and Challenges. *J. Phys. D: Appl. Phys.* **2011**, *44*, 303001.

(4) Kim, W.; Oh, S.-J.; Nahm, T.-H. Oxidation and Annealing Effect on Cobalt Films on Palladium (111). *Surf. Rev. Lett.* **2002**, *9*, 931−936.

(5) Martirosyan, K. S.; Zyskin, M. Reactive Self-heating Model of Aluminum Spherical Nanoparticles. *Appl. Phys. Lett.* **2013**, *102*, 053112.

(6) Terris, D. B.; Thomson, T.; Hu, G. Patterned Media for Future Magnetic Data Storage. *Microsyst. Technol.* **2007**, *13*, 189−196.

(7) Ross, C. A. Patterned Magnetic Recording Media. *Annu. Rev. Mater. Res.* **2001**, *31*, 203−235.

(8) Hu, B.; Amos, N.; Tian, Y.; Butler, J.; Litvinov, D.; Khizroev, S. Study of Co/Pd Multilayers as a Candidate Material for Next Generation Magnetic Media. *J. Appl. Phys.* **2011**, *109*, 034314.

(9) Lairson, B. M. Pd/Co Multilayers for Perpendicular Magnetic Recording. *IEEE Trans. Magn.* **1994**, *30*, 4014−4016.

(10) den Broeder, F. J. A.; Donkersloot, H. C.; Draaisma, H. J. G.; de Jone, W. J. M. Magnetic Properties and Structure of Pd/Co and Pd/Fe Multilayers. *J. Appl. Phys.* **1987**, *61*, 4317.

(11) Carcia, P. F.; Meinhaldt, A. D.; Suna, A. Perpendicular Magnetic Anisotropy in Pd/Co Thin Film Layered Structures. *Appl. Phys. Lett.* **1985**, *47*, 178−180.

(12) E, S.; Smith, D.; Svedberg, E.; Khizroev, S.; Litvinov, D. Combinatorial Synthesis of Co/Pd Magnetic Multilayers. *J. Appl. Phys.* **2006**, *99*, 113901.

(13) Bennett, W. R.; England, C. D.; Person, D. C.; Falco, C. M. Magnetic Properties of Pd/Co multilayers. *J. Appl. Phys.* **1991**, *69*, 4384−4390.

(14) Hashimoto, S.; Ochiai, Y.; Aso, K. Perpendicular Magnetic Anisotropy and Magnetostriction of Sputtered Co/Pd and Co/Pt Multilayered Films. *J. Appl. Phys.* **1989**, *66*, 4909−4916.

(15) Hobosyan, M. A.; Martirosyan, K. S. Consolidation of Lunar Regolith Simulant by Activated Thermite Reactions. *J. Aerosp. Eng.* **2014**, *10*, 1061.

(16) Atanassova, E.; Spassov, D. X-ray Photoelectron Spectroscopy of Thermal Thin Ta_2O_5 Films on Si. *Appl. Surf. Sci.* **1998**, *135*, 71.

(17) Atanassova, E.; Dimitrova, T.; Koprinarva, J. AEC and XPS Study of Thin RF-spttered Ta_2O_5 Layers. *Appl. Surf. Sci.* **1995**, *84*, 193.

(18) Demiryont, H.; Sites, J. R.; Geib, K. Effects of Oxygen Content on the Optical Properties of Tantalum Oxide Films Deposited by Ion-beam sputtering. *Appl. Opt.* **1985**, *24*, 490.

(19) Zier, M.; Oswald, S.; Reiche, R.; Wetzig, K. XPS Investigations of Thin Tantalum Films on a Silicon Surface. *Anal. Bioanal. Chem.* **2003**, *375*, 902.

(20) Lau, J. W.; McMichael, R. D.; Chung, S. H.; Rantschler, J. O.; Parekh, V.; Litvinov, D. Microstructural Origin of Switching Field Distribution in Patterned Co/Pd Multilayer Nanodots. *Appl. Phys. Lett.* **2008**, *92*, 01250.

(21) Kryder, M. H.; Cage, E. C.; McDaniel, T. W.; Challener, W. A.; Rottmayer, R. E.; Ju, G.; Hsia, Y.-T.; Erden, M. F. Heat Assisted Magnetic Recording. *Proc. IEEE* **2008**, *96*, 1810−1835.

(22) Rottmayer, R. E.; Batra, S.; Buechel, D.; Challener, W. A.; Hohlfeld, J.; Kubota, Y.; Li, L.; Lu, B.; Mihalcea, C.; Mountfield, K.; Pelhos, K.; Peng, C.; Rausch, T.; Seigler, M. A.; Weller, D.; Yang, X. Heat-Assisted Magnetic Recording. *IEEE Trans. Magn.* **2006**, *42*, 2417−2421.

(23) Seigler, M. A.; Challener, W. A.; Gage, E.; Gokemeijer, N.; Ju, G.; Lu, B.; Pelhos, K.; Peng, C.; Rottmayer, R. E.; Yang, X.; Zhou, H.; Rausch, T. Integrated Heat Assisted Magnetic Recording Head: Design and Recording Demonstration. *IEEE Trans. Magn.* **2008**, *44*, 119−124.

DOI: 10.1021/am5090463
ACS Appl. Mater. Interfaces 2015, 7, 6014−6018